JCI The Journal of Clinical Investigation

# $p21^{Cip1}$ modulates arterial wound repair through the stromal cell–derived factor-1/CXCR4 axis in mice

Michelle Olive, … , Jason C. Kovacic, Manfred Boehm

*J Clin Invest.* 2008;118(6):2050-2061. https://doi.org/10.1172/JCI31244.

**Research Article** **Vascular biology**

Cyclin-dependent kinase inhibitors, including $p21^{Cip1}$, are implicated in cell turnover and are active players in cardiovascular wound repair. Here, we show that $p21^{Cip1}$ orchestrates the complex interactions between local vascular and circulating immune cells during vascular wound repair. In response to femoral artery mechanical injury, mice with homozygous deletion of $p21^{Cip1}$ displayed accelerated proliferation of VSMCs and increased immune cell infiltration. BM transplantation experiments indicated that local $p21^{Cip1}$ plays a pivotal role in restraining excessive proliferation during vascular wound repair. Increased local vascular stromal cell–derived factor-1 (SDF-1) levels were observed after femoral artery injury in $p21^{+/+}$ and $p21^{-/-}$ mice, although this was significantly greater in $p21^{-/-}$ animals. In addition, disruption of SDF-1/CXCR4 signaling inhibited the proliferative response during vascular remodeling in both $p21^{+/+}$ and $p21^{-/-}$ mice. We provide evidence that the JAK/STAT signaling pathway is an important regulator of vascular SDF-1 levels and that $p21^{Cip1}$ inhibits STAT3 binding to the STAT-binding site within the murine SDF-1 promoter. Collectively, these results suggest that $p21^{Cip1}$ activity is essential for the regulation of cell proliferation and inflammation after arterial injury in local vascular cells and that the SDF-1/CXCR4 signaling system is a key mediator of vascular proliferation in response to injury.



# p21$^{Cip1}$ modulates arterial wound repair through the stromal cell–derived factor-1/CXCR4 axis in mice

Michelle Olive,[1] Jason A. Mellad,[2] Leilani E. Beltran,[2] Mingchao Ma,[2] Thomas Cimato,[2] Audrey C. Noguchi,[2] Hong San,[1] Richard Childs,[3] Jason C. Kovacic,[2] and Manfred Boehm[2]

[1]Genome Technology Branch, National Human Genome Research Institute, Bethesda, Maryland, USA. [2]Cardiovascular Branch and [3]Hematology Branch, National Heart, Lung, and Blood Institute, Bethesda, Maryland, USA.

**Cyclin-dependent kinase inhibitors, including p21$^{Cip1}$, are implicated in cell turnover and are active players in cardiovascular wound repair. Here, we show that p21$^{Cip1}$ orchestrates the complex interactions between local vascular and circulating immune cells during vascular wound repair. In response to femoral artery mechanical injury, mice with homozygous deletion of p21$^{Cip1}$ displayed accelerated proliferation of VSMCs and increased immune cell infiltration. BM transplantation experiments indicated that local p21$^{Cip1}$ plays a pivotal role in restraining excessive proliferation during vascular wound repair. Increased local vascular stromal cell–derived factor-1 (SDF-1) levels were observed after femoral artery injury in *p21*$^{+/+}$ and *p21*$^{-/-}$ mice, although this was significantly greater in *p21*$^{-/-}$ animals. In addition, disruption of SDF-1/CXCR4 signaling inhibited the proliferative response during vascular remodeling in both *p21*$^{+/+}$ and *p21*$^{-/-}$ mice. We provide evidence that the JAK/STAT signaling pathway is an important regulator of vascular SDF-1 levels and that p21$^{Cip1}$ inhibits STAT3 binding to the STAT-binding site within the murine SDF-1 promoter. Collectively, these results suggest that p21$^{Cip1}$ activity is essential for the regulation of cell proliferation and inflammation after arterial injury in local vascular cells and that the SDF-1/CXCR4 signaling system is a key mediator of vascular proliferation in response to injury.**

## Introduction

Vascular wound repair is controlled by the interaction of local vascular cells (endothelial and smooth muscle) and infiltrating inflammatory cells (macrophages, neutrophils, and lymphocytes). Particularly during arterial wound healing, a balanced control of vascular cell growth and death critically regulates the determination of both the composition of the healed arterial wall and luminal patency. Normally, during vascular homeostasis there is a low turnover rate of endothelial and smooth muscle cells. However, following arterial injury there is disruption of vessel architecture, triggering the early release of growth factors and inflammatory modulators that initiate a further cascade of downstream events (1, 2). Circulating inflammatory and progenitor cells are recruited to the site of injury and infiltrate the damaged vessel via the vessel lumen or the vasa vasorum, while previously quiescent local vascular cells also enter the cell cycle and proliferate (3). Although many cells participate in this early response to vascular injury, monocytes/macrophages have been noted as being particularly abundant (4). The recruitment of monocytes/macrophages is mediated by the chemokine stromal cell–derived factor-1 (SDF-1), which is upregulated at the site of tissue injury (5). SDF-1 is selectively bound by the chemokine receptor CXCR4, which is expressed on macrophages (6) and a wide range of other cells, including VSMCs (7, 8). CXCR4 signaling is mediated by G protein–dependent PI3K signal transduction pathways and the G protein–independent JAK/STAT pathway (9, 10).

The Cip/Kip proteins (p21$^{Cip1}$, p27$^{Kip1}$, and p57$^{Kip2}$) bind to and alter the activities of cyclin D–, cyclin E–, and cyclin A–dependent kinases in quiescent cells (11, 12). The cyclin-dependent kinase inhibitor (CKI) p21$^{Cip1}$ was initially identified as a potent inhibitor of cell cycle progression (13–16). Subsequent studies further identified that p21$^{Cip1}$ has an important role in controlling cytostasis and cell death (17). Interestingly, it has also been shown that at low levels, p21$^{Cip1}$ may have growth-permissive effects on cells by promoting the assembly of the CDK/cyclin D complex (18, 19). p21$^{Cip1}$ transcription is activated by p53, and p21$^{Cip1}$ is part of a negative feedback mechanism that controls p53 activity during apoptosis (20). p21$^{Cip1}$ has been shown to be an important mediator of inflammation, VSMC proliferation (21, 22), and vascular proliferative disease (23–27). Of particular relevance, p21 knockout mice have been shown to exhibit enhanced neointimal formation following arterial injury (28). Similarly, in models of vascular wound repair, p27$^{Kip1}$ has been shown to be an important modulator of vascular remodeling during the wound healing process (4, 29). Also, both p21$^{Cip1}$ and p27$^{Kip1}$ are known to be involved with the antiproliferative effects of sirolimus, a drug that is loaded onto "drug-coated" endovascular stents used in the treatment of ischemic heart disease (30–33).

Recently, p21$^{Cip1}$ was identified as not just a CKI, but also an important transcriptional regulator (34, 35). Thus, p21$^{Cip1}$ has been shown to regulate the activity of NF-κB, c-Myc, C/EBP, E2F, and STAT3 (36–39). The potential contribution of this aspect of p21$^{Cip1}$ activity during vascular wound repair is unknown. Interestingly, the apparent paradox that p21$^{Cip1}$ is not expressed in normal quiescent vessels but is upregulated in the proliferative phase of vascular remodeling may indicate an additional role besides the inhibition of cell cycle progression (40).

**Nonstandard abbreviations used:** LIF, leukemia inhibitory factor; SDF-1, stromal cell–derived factor-1.

**Conflict of interest:** The authors have declared that no conflict of interest exists.

**Citation for this article:** *J. Clin. Invest.* **118**:2050–2061 (2008). doi:10.1172/JCI31244.

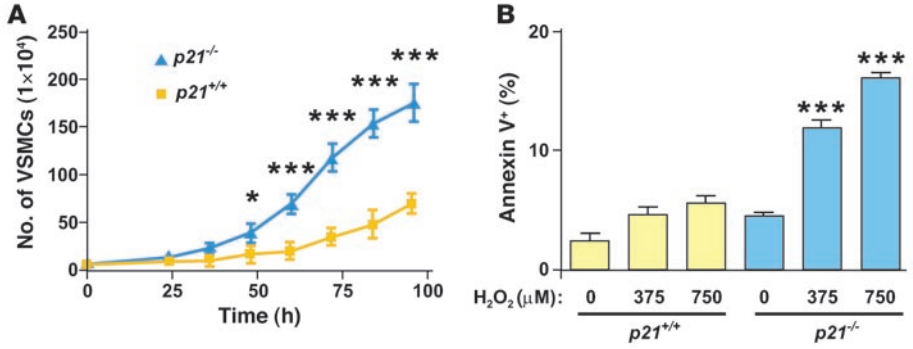


**Figure 1**
Accelerated proliferation and apoptosis in vitro in *p21*$^{-/-}$ VSMCs. (**A**) Increased growth rate in *p21*$^{-/-}$ VSMCs (blue triangles) compared with *p21*$^{+/+}$ VSMCs (yellow squares) ($n$ = 3; *$P$ < 0.05, ***$P$ < 0.001). (**B**) Increased percentage of apoptotic cells in *p21*$^{-/-}$ VSMCs (blue bars) induced with 0, 375, or 750 μM of $H_2O_2$ compared with *p21*$^{+/+}$ VSMCs (yellow bars) ($n$ = 3; ***$P$ < 0.001 versus corresponding *p21*$^{+/+}$ group).

The present study was undertaken to delineate the functions of p21$^{Cip1}$ in vascular and circulating inflammatory cells during arterial wound repair. Our results indicate that SDF-1/CXCR4 signaling mediates the local inflammatory and cellular proliferative response after arterial injury in WT mice and that blockade of this pathway leads to decreased neointimal formation. We provide evidence that p21$^{Cip1}$ has a particularly important role in restraining local levels of VSMC-derived SDF-1 and that after vascular injury, *p21*$^{-/-}$ mice show an increase in both SDF-1 expression and neointimal formation as compared with WT animals. In addition, we show that vascular SDF-1 is transcriptionally regulated through the JAK/STAT pathway as part of a positive feedback loop and that p21$^{Cip1}$ represses this process by binding to STAT3 and decreasing the STAT3-dependent transcriptional activation of the SDF-1.

Defining the roles of p21$^{Cip1}$ and SDF-1 in the vascular repair process provides essential information regarding their function in the development of cardiovascular disease and may assist in the development of novel strategies to ameliorate this condition.

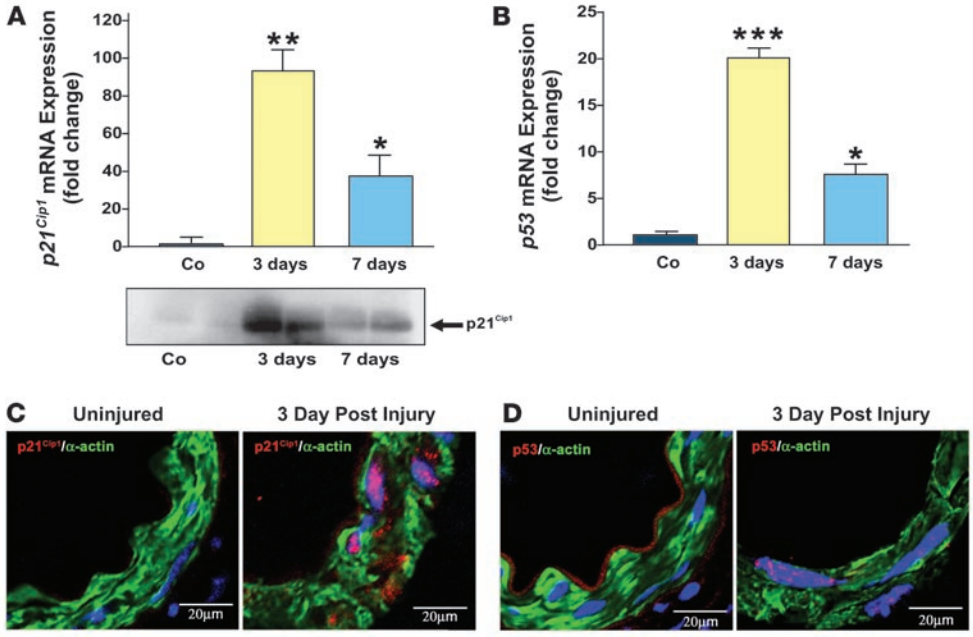


**Figure 2**
p21$^{Cip1}$ and p53 are induced after vascular injury. Vascular wire injury was performed on *p21*$^{+/+}$ mice, and femoral arteries were harvested 3 and 7 days following injury. (**A**) Upper panel: Total RNA was isolated from femoral arteries, and endogenous *p21*$^{Cip1}$ mRNA was quantified by quantitative PCR and normalized to levels of 18S RNA. Levels of *p21*$^{Cip1}$ mRNA at 3 (yellow bar) and 7 days (blue bar) are expressed relative to that measured in uninjured control (Co) arteries ($n$ = 3; *$P$ < 0.05 versus Co; **$P$ < 0.01 versus Co). Lower panel: Western blot analysis of p21$^{Cip1}$ levels in femoral arteries at 3 and 7 days after injury compared with uninjured arteries. (**B**) Levels of *p53* mRNA at 3 (yellow bar) and 7 days (blue bar) are expressed relative to that measured in uninjured arteries ($n$ = 3; *$P$ < 0.05 versus Co; ***$P$ < 0.001 versus Co). p21$^{Cip1}$ (**C**) and p53 (**D**) staining were detected by confocal microscopy in VSMCs arteries 3 days after injury. VSMCs were identified by smooth muscle α-actin (green), p21$^{Cip1}$ (**C**, red), p53 (**D**, red), and nuclear counterstaining by DAPI (blue). p21$^{Cip1}$ and p53 appear pink due to the overlay with the blue DAPI staining.

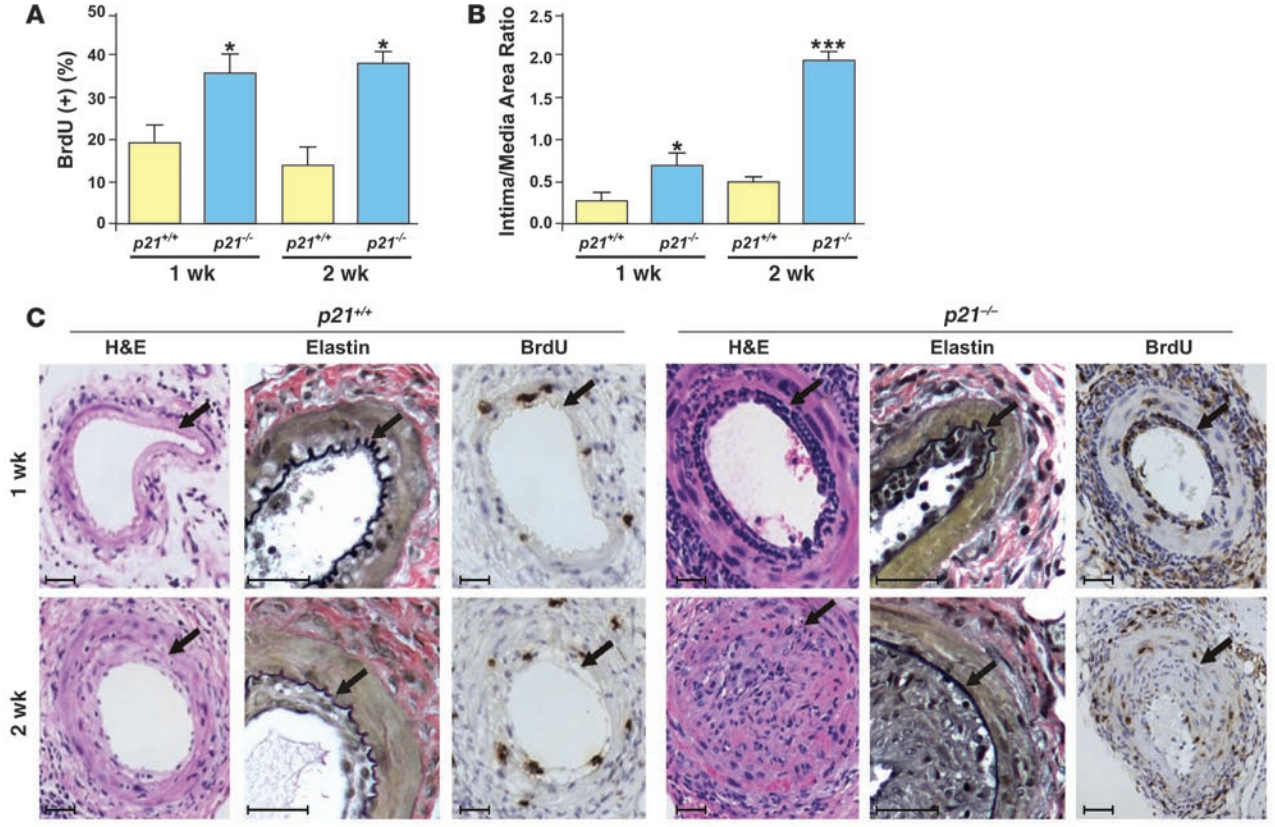


**Figure 3**
Impaired wound healing in $p21^{-/-}$ mice in vivo. (**A**) Increased cell proliferation was observed in $p21^{-/-}$ mice (blue bars) compared with $p21^{+/+}$ mice (yellow bars) at the 1- and 2-week time points after arterial injury ($n = 8$; $^{*}P < 0.05$ versus $p21^{+/+}$ at same time point) (**B**) Increased intima/media area ratio in $p21^{-/-}$ arteries (blue bars) compared with $p21^{+/+}$ arteries (yellow bars) following wire injury ($n = 8$; $^{*}P < 0.05$ versus $p21^{+/+}$ 1 wk, $^{***}P < 0.001$ versus $p21^{+/+}$ 2 wk). (**C**) Representative cross-sections of $p21^{+/+}$ (left) and $p21^{-/-}$ (right) arteries stained with H&E, elastin (black), and BrdU 1 and 2 weeks after injury. Arrows indicate the internal elastic lamina. Scale bars: 40 μm.

## Results

*Increased proliferation and apoptosis in $p21^{-/-}$ VSMCs.* $p21^{Cip1}$ is known to modulate apoptosis in several cell types, including endothelial cells, VSMCs, cardiomyocytes, and tumor cells (41–44). Therefore, we hypothesized that $p21^{Cip1}$ may modulate cellular proliferation and susceptibility to apoptosis during vascular wound repair, and we initially examined these cellular functions of $p21^{Cip1}$ in VSMCs. Low-passage $p21^{+/+}$ and $p21^{-/-}$ VSMCs were seeded in equal number, and cellular growth was recorded. After 96 hours, there were 2.5-fold more $p21^{-/-}$ than $p21^{+/+}$ VSMCs (Figure 1A), indicating that $p21^{-/-}$ VSMCs had a higher growth rate than $p21^{+/+}$ VSMCs. Next, cellular stress and apoptosis were induced by adding increasing concentrations of either $H_2O_2$ or FasL to the culture medium. In the absence of $H_2O_2$ or FasL, the percentage of apoptotic $p21^{-/-}$ and $p21^{+/+}$ VSMCs was similar (Figure 1B and Supplemental Figure 1; supplemental material available online with this article; doi:10.1172/JCI31244DS1). However, upon induction of cellular stress with increasing doses of $H_2O_2$ or FasL, the percentage of apoptotic cells increased significantly in the $p21^{-/-}$ group compared with the $p21^{+/+}$ group (Figure 1B and Supplemental Figure 1). These results confirm that $p21^{Cip1}$ supports cell viability during cellular stress and also inhibits VSMC proliferation.

*$p21^{Cip1}$ inhibits neointimal formation during arterial wound repair.* We used an established model of femoral artery wire injury to study the role of $p21^{Cip1}$ in the vascular repair process (45). First, we explored $p21^{Cip1}$ mRNA and protein levels in $p21^{+/+}$ mice during arterial wound repair. Quantitative PCR and western blot analyses revealed that both $p21^{Cip1}$ protein and mRNA levels were low in uninjured femoral arteries (Figure 2A). However, 3 days after vascular injury, $p21^{Cip1}$ protein and mRNA levels were markedly upregulated, the latter more than 90-fold (Figure 2A). $p21^{Cip1}$ mRNA subsequently decreased at later stages of the arterial repair process (Figure 2A). Since $p21^{Cip1}$ transcription is activated by p53, we explored p53 expression in the context of the vascular injury. We observed that *p53* mRNA levels followed the same pattern as $p21^{Cip1}$ mRNA. Thus, *p53* mRNA was near the limits of detection in uninjured vessels, but was elevated 20-fold 3 days after injury and subsequently decreased by 7 days after injury (Figure 2B). Confocal microscopic imaging confirmed the induction of nuclear $p21^{Cip1}$ and p53 expression in VSMCs within the medial arterial layer (Figure 2, C and D). These results suggest that $p21^{Cip1}$ may be at least partially regulated by p53 in the early phase of the vascular remodeling.

Next, we explored whether $p21^{Cip1}$ modulates arterial wound repair. We performed vascular injury in $p21^{-/-}$ and $p21^{+/+}$ mice and examined cell proliferation and lesion formation. Cell proliferation was determined by in vivo BrdU pulsing and was significantly increased within the neointima of $p21^{-/-}$ arteries compared with $p21^{+/+}$ arteries at 1 and 2 weeks after injury (Figure 3, A and C). Correspondingly, there was significantly greater neointimal for-

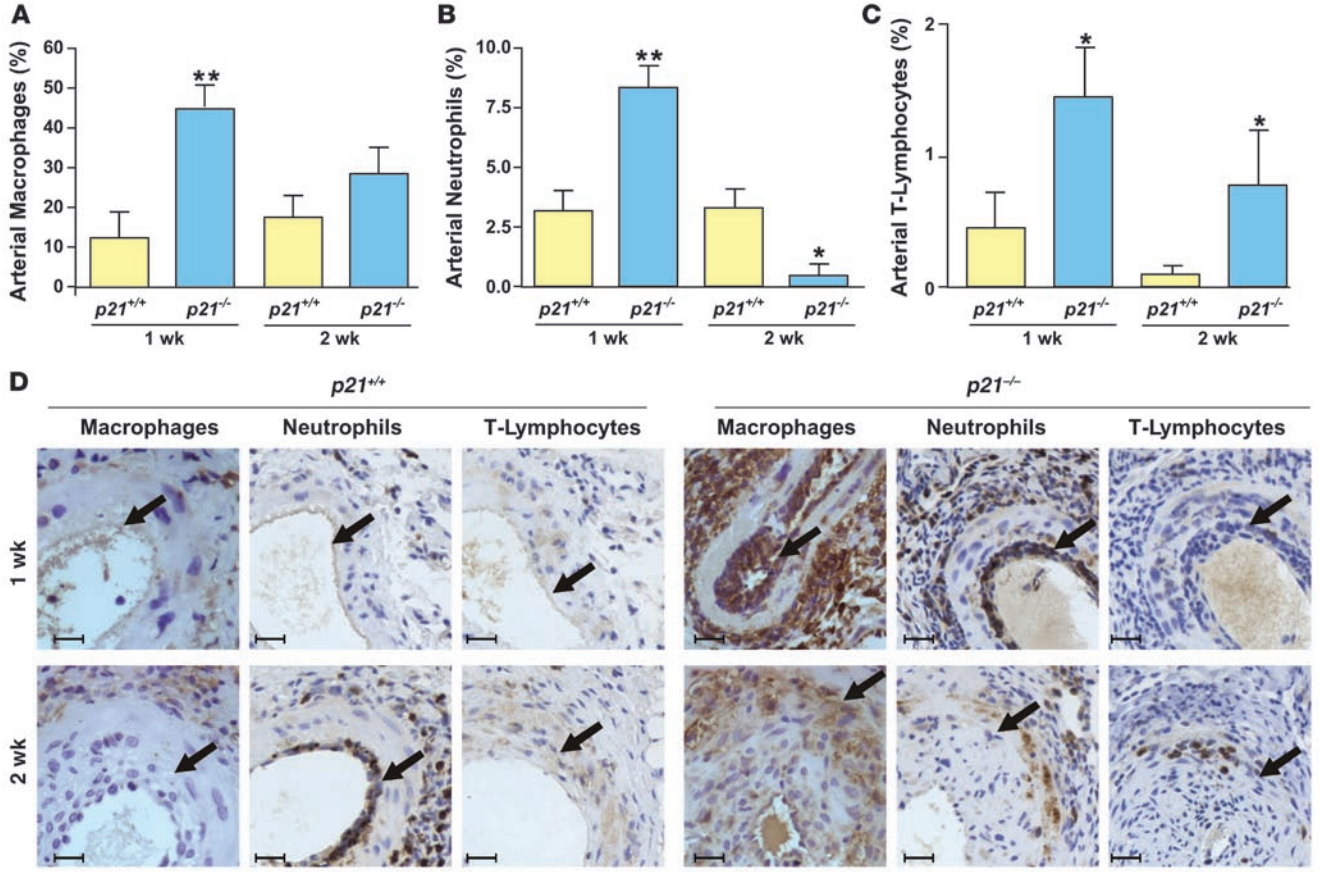


**Figure 4**

*p21*$^{-/-}$ mice develop acute arterial inflammation after vascular injury. Accumulation of (**A**) macrophages, (**B**) neutrophils, and (**C**) T lymphocytes in the femoral artery (neointima, media, and adventitia) of *p21*$^{+/+}$ (yellow bars) and *p21*$^{-/-}$ (blue bars) at 1 and 2 weeks after vascular injury ($n = 8$; $^{*}P < 0.05$ and $^{**}P < 0.01$ versus *p21*$^{+/+}$ at same time point). (**D**) Representative photomicrographs of cross-sections of *p21*$^{+/+}$ (left) and *p21*$^{-/-}$ (right) arteries immunostained for macrophages, neutrophils, and T lymphocytes (brown). Arrows indicate the internal elastic lamina. Scale bars: 20 μm.

mation in *p21*$^{-/-}$ mice when compared with *p21*$^{+/+}$ mice at both the 1- and 2-week time points (Figure 3, B and C). These observations confirm the role of p21$^{Cip1}$ in vascular wound repair and demonstrate that this process is greatly compromised in *p21*$^{-/-}$ mice compared with *p21*$^{+/+}$ mice.

*p21*$^{Cip1}$ *modulates the neointimal inflammatory response after vascular injury*. We noted a significant accumulation of mononuclear cells within the adventitia, media, and neointima after arterial injury and undertook further characterization of these cells. Histological sections were stained with antibodies specific for macrophages, neutrophils, and T lymphocytes at 1 and 2 weeks after injury (Figure 4). Compared with *p21*$^{+/+}$ mice, in *p21*$^{-/-}$ mice 1 week after injury, the number of macrophages in the adventitia, media, and neointima was 3.8-fold greater. However, there was no difference in macrophage counts 2 weeks after injury (Figure 4A). There were twice as many neutrophils in the lesions of *p21*$^{-/-}$ mice compared with *p21*$^{+/+}$ mice 1 week after arterial injury, but interestingly, this trend was reversed in the later phase of arterial wound repair (Figure 4B). In contrast, the number of T lymphocytes was increased in the lesions of *p21*$^{-/-}$ mice compared with those of *p21*$^{+/+}$ mice at both time points (Figure 4C). In summary, at the 1-week time point after arterial injury, all 3 inflammatory cells (macrophages, neutrophils, and T lymphocytes) were more abundant in the lesions of *p21*$^{-/-}$ mice than in those of *p21*$^{+/+}$ mice. However, p21$^{Cip1}$ deletion generally failed to sustain this enhanced inflammatory response in the later phase of arterial wound repair. Interestingly, we found no difference between *p21*$^{-/-}$ and *p21*$^{+/+}$ mice in the number of circulating inflammatory cells or the percentage of monocyte subtypes, at baseline and after wire injury (Supplemental Table 1 and Supplemental Figure 2, A and B). These data show that, particularly in the early phase of arterial wound repair, p21$^{Cip1}$ acts to decrease the migration and trafficking of inflammatory cells into areas of vascular damage.

*Vascular p21*$^{Cip1}$ *restrains excessive proliferation and decreases apoptosis during arterial wound repair*. To delineate the specific function of p21$^{Cip1}$ in local vascular cells versus that in circulating immune cells, we performed BM transplantation from *p21*$^{-/-}$ or *p21*$^{+/+}$ donors into *p21*$^{-/-}$ or *p21*$^{+/+}$ recipient mice. Successful engraftment was confirmed by the detection of the SRY gene in the blood of female recipients that received male BM by quantitative PCR (data not shown). Mice underwent vascular injury, and neointimal formation was determined 2 weeks later. When *p21*$^{-/-}$ mice received BM from *p21*$^{+/+}$ mice, neointimal formation was decreased compared to *p21*$^{-/-}$ mice that received *p21*$^{-/-}$ BM (Figure 5A). However, when *p21*$^{+/+}$ mice received BM from *p21*$^{-/-}$ mice, arterial wound repair was not altered, and neointimal formation was identical to that seen in *p21*$^{+/+}$ mice that received *p21*$^{+/+}$ BM (Figure 5A). These experiments indicate that

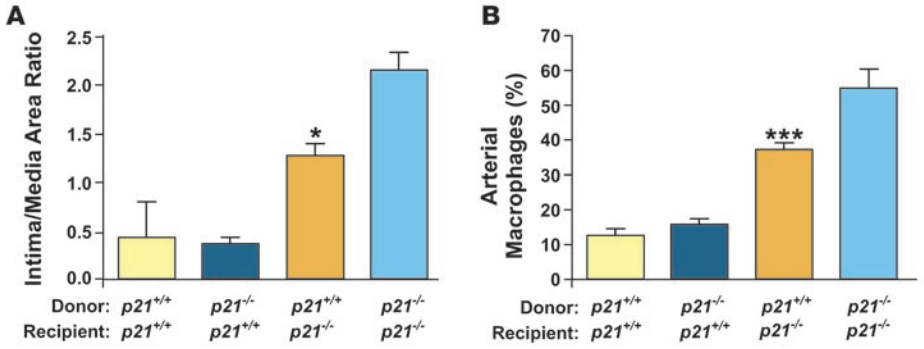


**Figure 5**

Local vascular p21$^{Cip1}$ modulates vascular wound repair. (**A**) BM transfer experiments were performed between *p21*$^{+/+}$ and *p21*$^{-/-}$ mice. Intima/media ratios were measured 2 weeks after vascular injury. The transplantation of *p21*$^{+/+}$ BM into *p21*$^{-/-}$ mice (orange bar) decreased arterial lesion formation compared with *p21*$^{-/-}$ BM transplanted into *p21*$^{-/-}$ mice (light blue bar) ($n = 8$; $^{*}P < 0.05$). (**B**) The percentage of arterial macrophages measured 7 days after injury was decreased in *p21*$^{-/-}$ mice that received *p21*$^{+/+}$ BM (orange bar) compared with mice that received *p21*$^{-/-}$ BM (light blue bar) ($n = 8$; $^{***}P < 0.001$). This effect was not seen in *p21*$^{+/+}$ mice, where the percentage of arterial macrophages was not different between mice that received *p21*$^{+/+}$ BM (yellow bar) and *p21*$^{-/-}$ BM (dark blue bar).

local vascular p21$^{Cip1}$ is sufficient to restrain excessive neointimal formation. In addition, p21$^{Cip1}$ deletion in local vascular cells caused increased infiltration of monocytes/macrophages (Figure 5B).

We then determined the influence of p21$^{Cip1}$ expression on apoptosis during arterial wound repair. Using a TUNEL assay, we found that at 1 week after arterial injury the percentage of apoptotic cells was significantly increased in *p21*$^{-/-}$ mice compared with *p21*$^{+/+}$ mice, although this difference was not sustained at 2 weeks after injury (Supplemental Figure 3A). In BM transplantation experiments 1 week after injury, transplantation of *p21*$^{-/-}$ BM into *p21*$^{+/+}$ recipients did not significantly increase the percentage of vascular apoptotic cells compared with *p21*$^{+/+}$ mice receiving *p21*$^{+/+}$ BM. Also, transplantation of *p21*$^{+/+}$ BM into *p21*$^{-/-}$ recipient mice did not significantly decrease this process compared with transplantation of *p21*$^{-/-}$ BM into *p21*$^{-/-}$ recipient mice (Supplemental Figure 3B). Thus, p21$^{Cip1}$ within local vascular cells appears to influence apoptosis after vascular injury, supporting the importance of local p21$^{Cip1}$ function in vascular wound repair.

As a whole, these observations led us to question what distinguishes local *p21*$^{+/+}$ from *p21*$^{-/-}$ vascular cells, and in particular, what factors might mediate the interactions of these resident vascular cells with circulating immune and inflammatory cells.

*Local vascular p21$^{Cip1}$ modulates SDF-1 during vascular wound repair.* As SDF-1 is known to play an important role in recruiting and detaining inflammatory cells at the site of vascular injury (5, 46), we speculated that local vascular SDF-1 may be differentially regulated in *p21*$^{-/-}$ versus *p21*$^{+/+}$ mice. Initial in vitro experiments confirmed increased protein levels of SDF-1 in *p21*$^{-/-}$ versus *p21*$^{+/+}$ VSMCs. After the induction of oxidative stress with $H_2O_2$, SDF-1 levels were significantly reduced in both *p21*$^{-/-}$ and *p21*$^{+/+}$ VSMCs (Supplemental Figure 4). Moving to our in vivo models, we first established that serum SDF-1 levels did not differ, before or 3 and 7 days after vascular injury, between *p21*$^{+/+}$ and *p21*$^{-/-}$ mice (data not shown). We then proceeded to investigate local vascular SDF-1 levels at these time points. In the absence of arterial injury, there was no difference in SDF-1 tissue levels between *p21*$^{+/+}$ and *p21*$^{-/-}$ mice. After injury, both *p21*$^{+/+}$ and *p21*$^{-/-}$ mice exhibited increased local SDF-1 levels compared with uninjured controls. However, in *p21*$^{-/-}$ mice this increase both was of a greater magnitude and also, unlike *p21*$^{+/+}$ mice, was sustained until at least 7 days after injury (Figure 6, A and B). In order to further explore this observation, local vascular SDF-1 levels were also measured in *p21*$^{+/+}$ and *p21*$^{-/-}$ mice that had undergone BM transplantation. Local SDF-1 was upregulated in *p21*$^{-/-}$ mice that received p*21*$^{+/+}$ BM compared with *p21*$^{+/+}$ mice that received *p21*$^{+/+}$ BM. In addition, *p21*$^{+/+}$ mice receiving *p21*$^{-/-}$ BM had similar levels of SDF-1 compared with *p21*$^{+/+}$ mice that received *p21*$^{+/+}$ BM (Figure 6C). These results indicate that p21$^{Cip1}$ expression (or lack thereof) by BM-derived cells has minimal influence on vascular SDF-1 levels after injury, and that it is local p21$^{Cip1}$ expression that modulates vascular SDF-1 levels.

*Inhibition of SDF-1/CXCR4 signaling restrains excessive proliferation during vascular wound repair in p21*$^{-/-}$ *mice.* Our results presented above suggest an important role for local vascular p21$^{Cip1}$ in the modulation of vascular SDF-1 levels. However, while SDF-1 has been implicated in the regulation of cellular migration in this (femoral artery wire injury) and other situations (47), the precise anatomical localization of SDF-1 during wound repair, at a cellular level, is not well described. We explored SDF-1 expression by immunohistochemistry in uninjured vessels and during the early phase of vascular wound repair. As indicated by double staining for VSMC-specific α-actin and SDF-1, in uninjured *p21*$^{+/+}$ and *p21*$^{-/-}$ murine femoral arteries, SDF-1 was predominantly expressed by VSMCs (Figure 6A). We did not observe significant staining in the endothelial cell layer (double staining for CD31 and SDF-1) or in the adventitia. This pattern of vascular SDF-1 expression was not altered by arterial injury. In addition, we did not detect obvious SDF-1 staining in either CD45-positive inflammatory cells, or F4/80-positive macrophages (Figure 6A and data not shown).

SDF-1 signaling is mediated via the CXCR4 receptor, which is commonly expressed on immune and vascular cells. We hypothesized that apart from playing an important role in WT animals, inhibition of SDF-1 signaling would reverse the hyperproliferative phenotype in *p21*$^{-/-}$ mice. We utilized 2 independent approaches to inhibit SDF-1/CXCR4 function. First, we administered AMD3100, a specific CXCR4 inhibitor, to *p21*$^{+/+}$ and *p21*$^{-/-}$ mice via osmotic minipumps and examined the inflammatory response and neointimal formation 1 and 2 weeks after vascular injury. Next, we inhibited the SDF-1/CXCR4 signaling pathway by treatment with a neutralizing monoclonal antibody against CXCR4 (48). As shown in Figure 7, A and B, the inhibition of SDF-1/CXCR4 signaling by either approach significantly reduced neointimal formation after vascular injury in *p21*$^{-/-}$ mice. CXCR4 blocking antibody also significantly inhibited neointimal formation in *p21*$^{+/+}$ mice (Figure 7B). However, possibly due to the additional early BM cell–mobilizing effect of AMD3100 and consistent with other reports (49), we observed that in *p21*$^{+/+}$ mice this reduction was only significant at the 2-week time point (Figure 7A). Cellular proliferation, as assessed by BrdU incorporation,

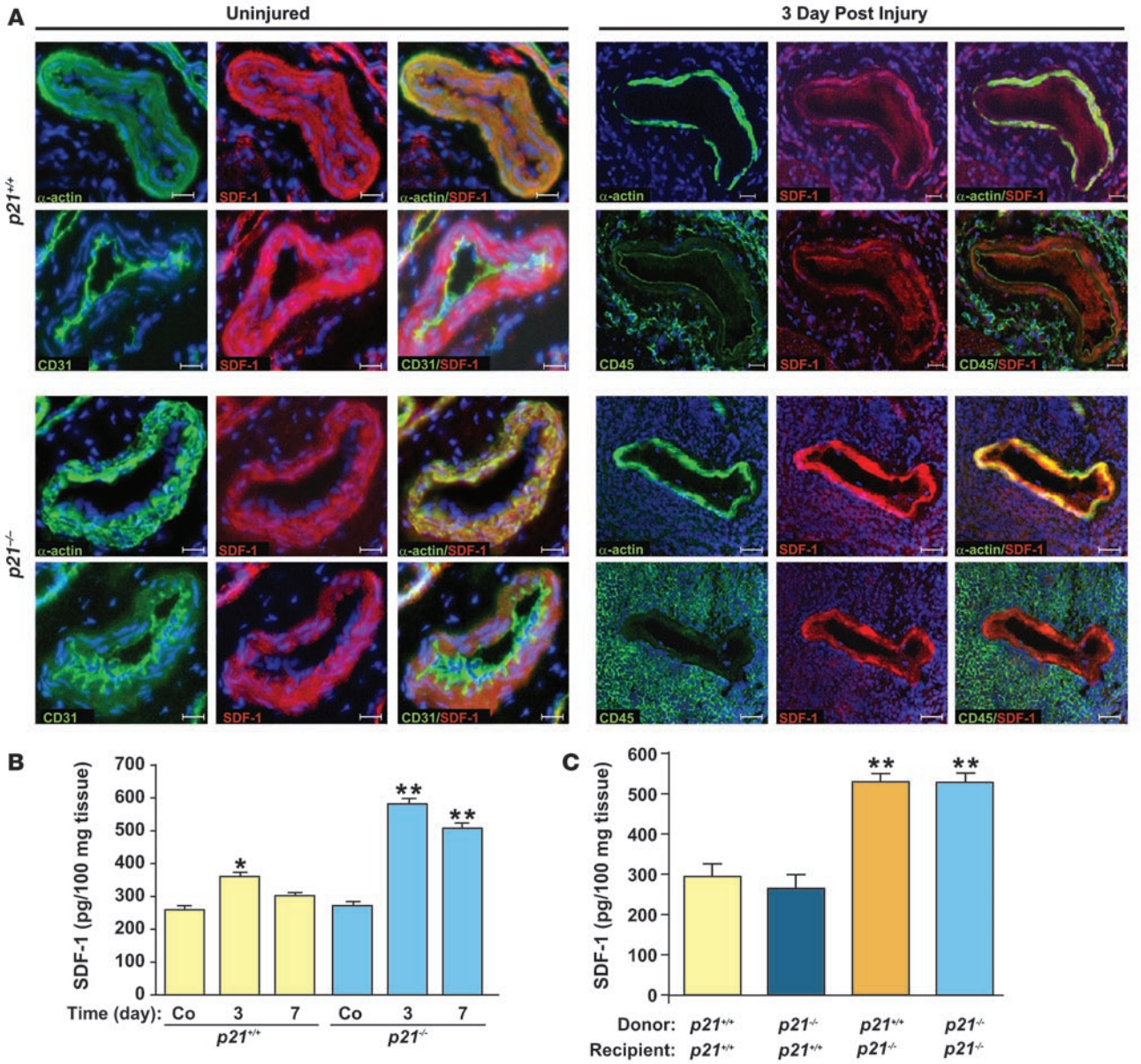


**Figure 6**

SDF-1 is localized to the arterial media, and SDF-1 tissue levels are increased in $p21^{-/-}$ mice receiving $p21^{+/+}$ BM after arterial injury. (**A**) SDF-1 staining in uninjured arteries (left panels) and in arteries 3 days after injury (right panels) from $p21^{+/+}$ (upper panels) and $p21^{-/-}$ (lower panels) mice. VSMCs were identified by smooth muscle α-actin (in green), endothelial cells by CD31 (in green), and inflammatory cells by CD45 (in green). SDF-1 staining is represented in red, and nuclei were counterstained by DAPI (blue). For uninjured and injured groups, left and middle columns represent individual staining; right columns are merged images. Scale bars: 40 μm. (**B**) Increased arterial tissue SDF-1 levels were observed in $p21^{-/-}$ (blue bars) compared with $p21^{+/+}$ mice (yellow bars) 3 and 7 days after injury ($n = 3$; $^{**}P < 0.01$ versus $p21^{+/+}$ at same time point). Increased SDF-1 levels were also observed in $p21^{+/+}$ mice 3 days after injury compared with uninjured $p21^{+/+}$ mice ($n = 3$; $^{*}P < 0.05$). (**C**) Arterial SDF-1 levels measured 7 days after injury were increased in $p21^{-/-}$ mice that received either $p21^{+/+}$ (orange bar) or $p21^{-/-}$ (light blue bar) BM compared with $p21^{+/+}$ mice that received either $p21^{+/+}$ (yellow bar) or $p21^{-/-}$ (dark blue bar) BM, respectively ($n = 5$; $^{**}P < 0.01$).

was significantly decreased by both CXCR4 blocking antibody and AMD3100 in $p21^{-/-}$ and $p21^{+/+}$ mice at 1 and 2 weeks after vascular injury (Figure 7C and Supplemental Figure 5A). We further identified that either approach to inhibiting SDF-1/CXCR4 signaling was associated with reduced macrophage infiltration at 1 and 2 weeks after vascular injury in both $p21^{-/-}$ and $p21^{+/+}$ mice (Figure 7D and Supplemental Figure 5B). In contrast, neither CXCR4 blocking antibody nor AMD3100 administration altered cellular apoptosis in $p21^{-/-}$ or $p21^{+/+}$ mice after vascular injury (Figure 7E and Supplemental Figure 5C). Interestingly, 1 week after vascular injury, $p21^{-/-}$ mice displayed a marginal increase in local vascular SDF-1 levels after treatment with AMD3100. However, this treatment did not influence vascular SDF-1 levels in $p21^{+/+}$ mice (Supplemental Figure 5D). Overall, these data confirmed the important influence of $p21^{Cip1}$ on the SDF-1/CXCR4 signaling pathway during vascular remodeling.

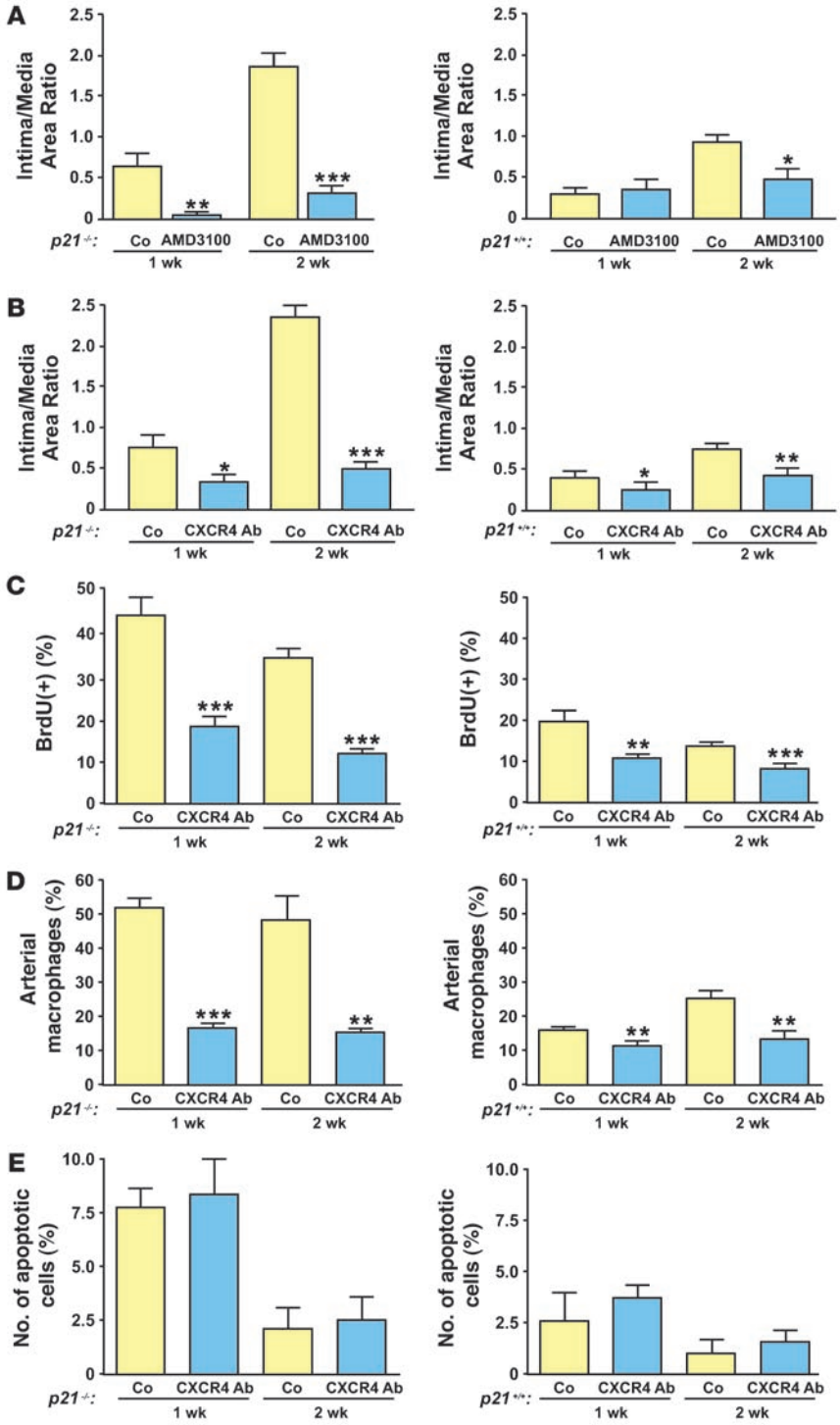


**Figure 7**
SDF-1 inhibition prevents excessive proliferation during vascular wound repair. (**A**) Reduced vascular lesions in *p21*$^{-/-}$ (left) and *p21*$^{+/+}$ arteries (right) after AMD3100 treatment compared with saline-treated animals (Co) 1 and 2 weeks after vascular injury (left, $n = 5$; right, $n = 10$). (**B**) Reduced vascular lesions in *p21*$^{-/-}$ and *p21*$^{+/+}$ arteries with anti-CXCR4–blocking antibody compared with mice treated with IgG control (left, $n = 5$; right, $n = 16$). (**C**) Anti-CXCR4 blocking antibody decreased cellular proliferation as assessed by BrdU incorporation at 1 and 2 weeks after vascular injury in *p21*$^{-/-}$ and *p21*$^{+/+}$ arteries (left, $n = 5$; right, $n = 5$). (**D**) Anti-CXCR4 blocking antibody reduced the number of local arterial macrophages in *p21*$^{-/-}$ and *p21*$^{+/+}$ arteries at 1 and 2 weeks after vascular injury (left, $n = 5$; right, $n = 5$). (**E**) The number of local apoptotic TUNEL-positive cells after vascular injury was unchanged after treatment with anti-CXCR4 blocking antibody. $^{*}P < 0.05$, $^{**}P < 0.01$, and $^{***}P < 0.001$ versus Co at same time point.

*p21*$^{Cip1}$ *regulates SDF-1 via the JAK-STAT signaling pathway*. We then investigated the mechanism whereby p21$^{Cip1}$ modulates SDF-1 levels. Recent publications suggest that p53 represses SDF-1 and its receptor CXCR4 as part of a negative regulatory loop (50, 51). We hypothesized that p21$^{Cip1}$ might also play an important role in this pathway and connect the cellular stress repair program to the inflammatory response. We screened the murine SDF-1 promoter region for possible transcription factors associated with p21$^{Cip1}$ and were able to localize a putative STAT binding site (–516/–527 in the murine SDF-1 promoter region). This was consistent with previous reports that JAK/STAT is an important mediator of SDF-1/CXCR4 signaling (9) and that STAT3 is a major transcriptional activator of SDF-1 and may also act upstream of SDF-1 by modulating HIF-1α activity (52). We initially explored the potential p21$^{Cip1}$/STAT3/SDF-1 interactions in primary murine VSMCs. A luciferase construct containing the –2,200-bp SDF-1 promoter sequence was transfected into *p21*$^{+/+}$ and *p21*$^{-/-}$ VSMCs. As shown in Figure 8A, this transfection resulted in a significant increase in SDF-1 promoter activity in *p21*$^{-/-}$ compared with *p21*$^{+/+}$ VSMCs.

Next, we explored whether activation or inhibition of the STAT3 binding site within the SDF-1 promoter serves to modulate the expression of SDF-1 in VSMCs. After serum starvation of VSMCs for 24 hours, *p21*$^{-/-}$ VSMCs exhibited a 3-fold increase in *SDF-1* mRNA expression compared with *p21*$^{+/+}$ VSMCs (Figure 8B). Subsequently, the addition of leukemia inhibitory factor (LIF), which is known to activate STAT3 (53), to the culture medium caused a further increase in *SDF-1* mRNA expression (Figure 8B). This activation was blocked by the cell membrane–permeable STAT3 inhibitor PpYLKTK-mts (Figure 8B). We then mutated the STAT3 binding site of our luciferase construct of the SDF-1 promoter sequence by a 4-bp substitution-mutation of the STAT3 binding site and transfected it into *p21*$^{+/+}$ and *p21*$^{-/-}$ VSMCs. As shown in Figure 8C, this caused a significant decrease in luciferase activity in both *p21*$^{+/+}$ and *p21*$^{-/-}$ cells compared with transfection with the nonmutated SDF-1 promoter construct. Further experiments also demonstrated that

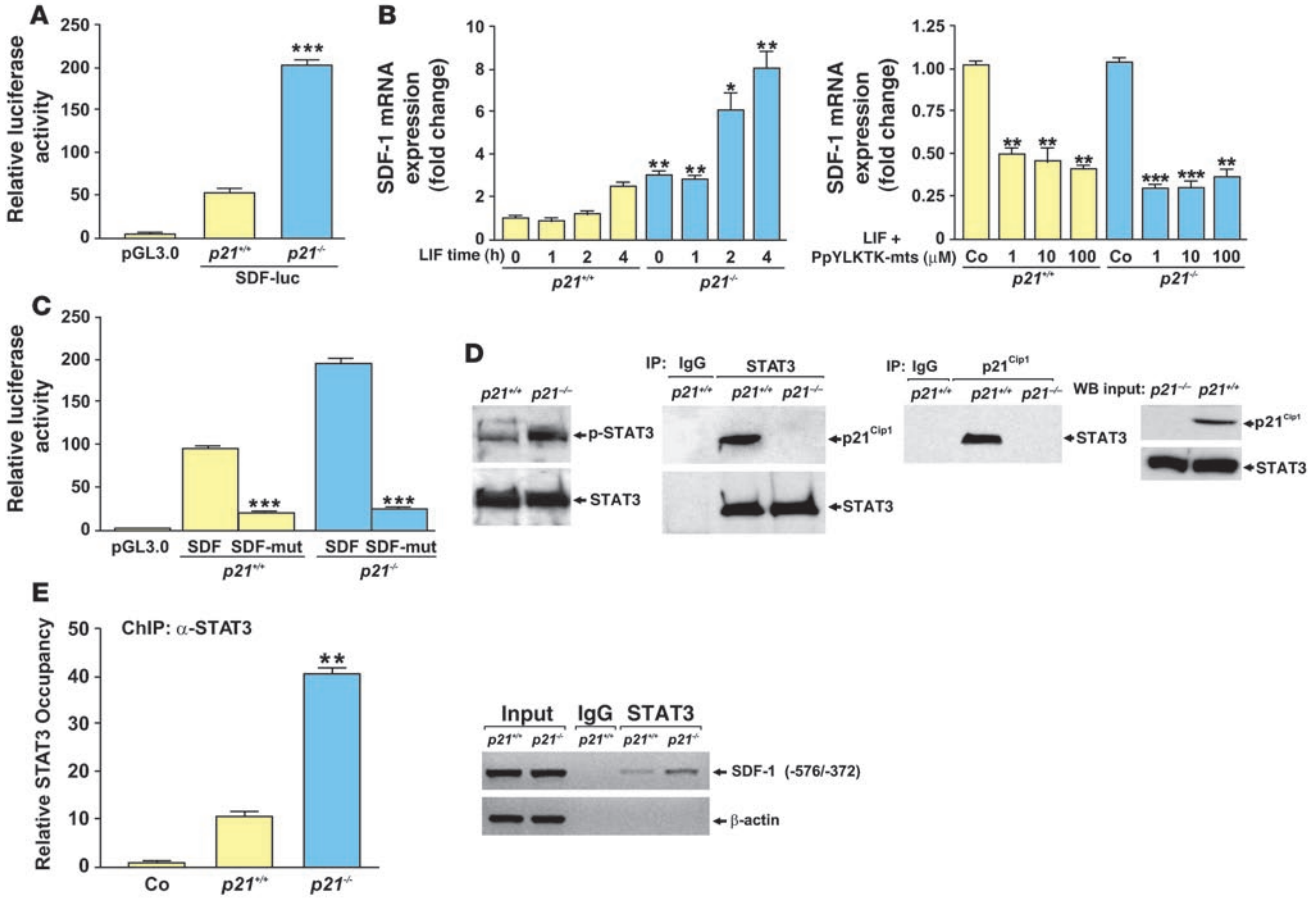


**Figure 8**

p21$^{Cip1}$ stimulates SDF-1 via STAT3 in VSMCs. (**A**) SDF-1 promoter activity is increased in *p21*$^{-/-}$ compared with *p21*$^{+/+}$ VSMCs (pGL3.0, backbone vector) ($n = 3$; ***$P < 0.001$). (**B**) Left: *SDF-1* mRNA levels are elevated at baseline and in LIF-stimulated cells (40 ng/ml) in *p21*$^{-/-}$ compared with *p21*$^{+/+}$ VSMCs. Results are expressed as fold activation compared with untreated (Co) *p21*$^{+/+}$ VSMCs ($n = 3$; *$P < 0.05$, **$P < 0.01$ compared with *p21*$^{+/+}$ at same time point). Right: Inhibition of STAT3 with PpYLKTK-mps at 1, 10, and 100 μM decreased *SDF-1* mRNA expression. Results are presented as fold activation compared with untreated *p21*$^{+/+}$ and *p21*$^{-/-}$ VSMCs ($n = 3$; *$P < 0.05$, **$P < 0.01$, ***$P < 0.001$). (**C**) Mutation of the STAT3 binding site in the SDF-1 promoter (SDF-mut) decreased luciferase activity compared with unmutated SDF-1 promoter (SDF) in *p21*$^{+/+}$ and *p21*$^{-/-}$ VSMCs ($n = 3$; ***$P < 0.001$). (**D**) Far left: Western blot analysis of p-STAT3 in *p21*$^{-/-}$ compared with *p21*$^{+/+}$ VSMC extracts. Middle (2 panels): p21$^{Cip1}$ interacts with STAT3 in *p21*$^{+/+}$ VSMC extracts. p21$^{Cip1}$ is pulled down by anti-STAT3 antibody, and STAT3 is pulled down by anti-p21$^{Cip1}$ antibody. Far right: p21$^{Cip1}$ and STAT3 inputs for the IP experiments. (**E**) ChIP from *p21*$^{+/+}$ and *p21*$^{-/-}$ VSMC chromatin extracts using anti-STAT3 antibody. Left: Quantification of STAT3 occupancy in the SDF-1 promoter region in *p21*$^{+/+}$ and *p21*$^{-/-}$ VSMCs ($n = 3$; **$P < 0.01$ versus *p21*$^{+/+}$). Right: PCR amplification of the SDF-1 (–576/–372 bp) and β-actin promoters after ChIP with control IgG or anti-STAT3 antibodies.

increased STAT3 activation through Tyr705 phosphorylation was present in *p21*$^{-/-}$ VSMCs compared with *p21*$^{+/+}$ VSMCs, and reciprocal coimmunoprecipitation experiments in VSMCs revealed an interaction between p21$^{Cip1}$ and STAT3 (Figure 8D).

Finally, we investigated whether STAT3 occupancy of the SDF-1 promoter is increased in *p21*$^{-/-}$ compared with *p21*$^{+/+}$ VSMCs. This was achieved by analyzing the chromatin of human VSMCs by ChIP using primers that flank the –576/–372 region of the SDF-1 promoter that we previously identified as being likely to contain a STAT3 binding site (see above). PCR analysis of the chromatin immunoprecipitates, isolated with anti-STAT3 antibodies, showed increased STAT3 occupancy of the SDF-1 promoter in *p21*$^{-/-}$ compared with *p21*$^{+/+}$ VSMCs (Figure 8E). These findings indicate that, at least in vitro, p21$^{Cip1}$ is likely to influence SDF-1 levels in VSMCs by modulating STAT3 transcriptional activity. To further explore this possibility in vivo, we performed a ChIP assay on femoral arteries from *p21*$^{-/-}$ and *p21*$^{+/+}$ mice at both 3 and 7 days after vascular injury. We observed an enhanced and prolonged STAT3 occupancy of the SDF-1 promoter in vessels from *p21*$^{-/-}$ mice compared with vessels from *p21*$^{+/+}$ mice (Figure 9, A and B). In summary, these data suggest that p21$^{Cip1}$ modulates the inflammatory response and SDF-1 through the JAK/STAT signal transduction pathway in vitro and in vivo during vascular wound repair.

## Discussion

Arterial wound repair is a complex process involving predominantly local vascular cells and circulating inflammatory cells. Despite the fact that this process is directly implicated in the etiology of clinical ischemic heart disease, the precise functioning of the relevant inter- and intracellular signaling pathways is not entirely understood (54, 55). Here, we provide direct evidence that p21$^{Cip1}$ plays a central role in vascular repair after injury. In brief, the major new findings to

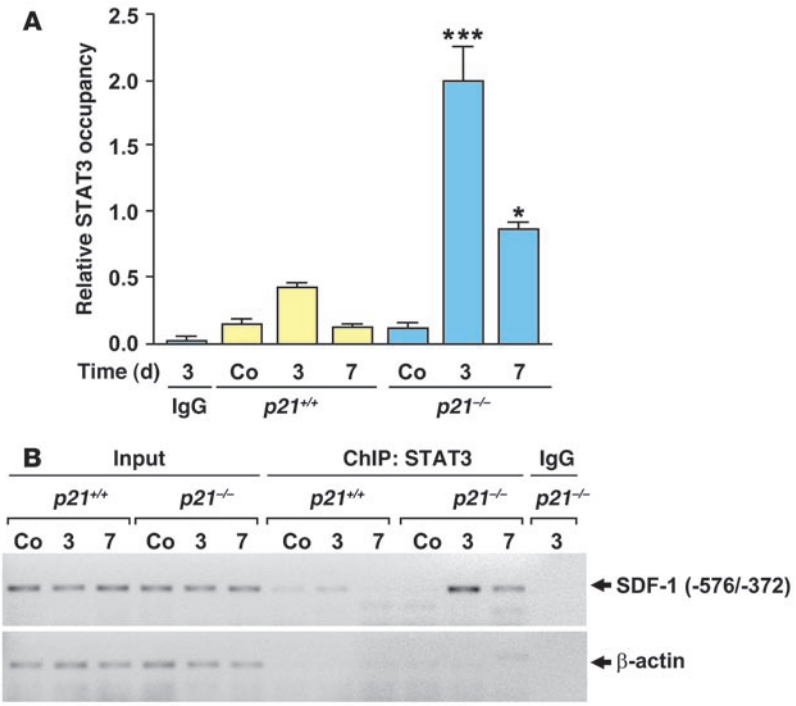


**Figure 9**
STAT3-dependent SDF-1 signaling pathway is impaired in the *p21*$^{-/-}$ arterial wall. ChIP assays on *p21*$^{+/+}$ and *p21*$^{-/-}$ femoral arteries using anti-STAT3 antibodies were performed before femoral wire injury (Co) and 3 and 7 days after injury. (**A**) Quantification of STAT3 occupancy within the SDF-1 promoter region in *p21*$^{+/+}$ and *p21*$^{-/-}$ femoral arteries ($n = 5$; $^{*}P < 0.05$, $^{***}P < 0.001$ versus same time point for *p21*$^{+/+}$). As a control, chromatin from *p21*$^{-/-}$ arteries 3 days after injury was immunoprecipitated with IgG. (**B**) PCR amplification of the SDF-1 (–572/–372 bp) and β-actin promoters after ChIP with IgG or anti-STAT3 antibodies following vascular injury.

arise from this work are as follows: (a) Deletion of p21$^{Cip1}$ enhances the inflammatory response during vascular wound repair. (b) Within medial VSMCs, p21$^{Cip1}$ restrains SDF-1 levels in the early phase of vascular remodeling. (c) Inhibition of SDF-1/CXCR4 signaling by the CXCR4-specific receptor antagonist AMD3100, or a CXCR4-blocking monoclonal antibody, acts to limit inflammation and neointimal formation in *p21*$^{+/+}$ and *p21*$^{-/-}$ mice during vascular wound repair. (d) VSMC-derived SDF-1 is transcriptionally regulated by the JAK/STAT signaling pathway. (e) p21$^{Cip1}$ modulates the occupancy of STAT3 on the SDF-1 promoter in VSMCs both in vitro and in vivo during vascular remodeling.

p21$^{Cip1}$ is acknowledged as being a key inhibitory regulator of cellular proliferation and a mediator of p53-dependent cellular apoptosis (35) and is considered to be a fundamental player in vascular wound repair (21, 23, 24, 26). To date, supporting evidence has included the observation that overexpression of recombinant p21$^{Cip1}$ decreases VSMC proliferation and attenuates the progression of vascular proliferative diseases (21, 23, 24, 26) and that, conversely, reduced p21$^{Cip1}$ expression leads to increased neointimal formation following arterial injury (28). This has led to the evaluation of novel treatment strategies for these diseases that are at least partially mediated through p21$^{Cip1}$ upregulation (25, 56, 57). Our results further extend this work and serve to reinforce the important role of p21$^{Cip1}$ in modulating vascular wound repair. We now additionally show that the hyperproliferative phenotype seen in *p21*$^{Cip1-/-}$ mice is associated with an increased number of inflammatory macrophages in the early phase of vascular wound repair. While other researchers have investigated this phenomenon in different settings, our findings are broadly consistent with the fact that p21$^{Cip1}$ plays an important role in regulating cell proliferation and monocyte/macrophage differentiation (21, 22). However, BM transplantation experiments demonstrated that the enhanced neointimal formation that was observed in *p21*$^{-/-}$ mice could not be recapitulated by transplanting *p21*$^{-/-}$ BM into *p21*$^{+/+}$ mice. Collectively, our experiments suggest that the hyperproliferative vascular phenotype of *p21*$^{-/-}$ mice is largely independent of BM-derived cells, but rather arises from the effects of p21$^{Cip1}$ on the local vascular milieu. Interestingly, this latter finding is in direct opposition to the situation with p27$^{Kip1}$, which primarily exerts its effects on arterial wound repair through infiltrating BM-derived immune cells (4).

Vascular wound repair is orchestrated by various cytokines and inflammatory mediators. While local SDF-1 levels were increased after vascular injury in *p21*$^{+/+}$ mice, we observed that *p21*$^{-/-}$ mice exhibit a significantly greater increase in local SDF-1 levels after arterial injury. This finding was not recapitulated by transplanting *p21*$^{-/-}$ BM into *p21*$^{+/+}$ mice, again suggesting that the effect of p21$^{Cip1}$ is at the local vascular level. These results also implicated p21$^{Cip1}$ in the regulation of SDF-1, and we therefore explored these potential interrelationships within the context of vascular wound repair. This was achieved by abrogating SDF-1/CXCR4 signaling using either the selective CXCR4 receptor antagonist AMD3100 (58) or a monoclonal antibody directed against CXCR4. Strengthening our hypothesis that p21$^{Cip1}$ is involved with SDF-1 regulation, we found that either approach led to decreased neointimal formation in both *p21*$^{+/+}$ and *p21*$^{-/-}$ mice. However, perhaps due to their higher degree of neointimal formation, we found that *p21*$^{-/-}$ mice exhibited a greater reduction in neointimal formation after SDF-1/CXCR4 blockade than did *p21*$^{+/+}$ animals.

Numerous publications have described a central role for the SDF-1/CXCR4 axis in new vessel formation, vascular wound repair, and VSMC proliferation (5, 48, 59–63). Zernecke et al. (63) found that the transplantation of CXCR4$^{-/-}$ fetal liver cells into *ApoE*$^{-/-}$ mice resulted in a greater than 50% reduction in neointimal area after vascular wire injury, suggesting a regulatory role for inflammatory and/or immune cells in wound repair and VSMC proliferation. Similarly, Grunewald et al. (5) reported that tissue-specific hepatic and cardiac VEGF overexpression stimu-

lated SDF-1 expression in perivascular "fibroblastic or smooth muscle" cells, which was sufficient to recruit and retain circulating $CD45^+CD11b^+CXCR4^+$ myeloid cells. These investigators also demonstrated that the induction of perivascular SDF-1 expression is an integral aspect of angiogenesis and that the administration of a CXCR4 antagonist significantly inhibits this process (5). Recently, SDF-1 was also shown to be an important downstream mediator of HIF-1α, both of which were found to be upregulated during the hyperproliferative response to vascular wire injury in *ApoE*$^{-/-}$ mice (64). Our results corroborate these publications, and we similarly found that SDF-1/CXCR4 signaling is of importance in both *p21*$^{-/-}$ and *p21*$^{+/+}$ mice. However, we further expand these intricate regulatory networks and suggest that $p21^{Cip1}$ is an important mediator of SDF-1 transcription.

$p21^{Cip1}$ is known to be a direct modulator of several transcription factors including STAT3 (34, 35, 37). We investigated this relationship in the context of SDF-1 transcription and were able to identify a putative STAT3-binding site within the murine SDF-1 promoter region. We also demonstrated that in VSMCs, activation of STAT3 signaling increases SDF-1 expression and, conversely, that inhibition of STAT3 signaling decreases SDF-1. In addition, we performed ChIP experiments on VSMCs and found that STAT3 occupancy could be detected on the SDF-1 promoter. Although SDF-1 was described as signaling through the JAK/STAT pathway almost a decade ago (9), we are unaware of any previous reports describing this reciprocal signaling arrangement, whereby the JAK/STAT pathway regulates SDF-1 transcription.

Integrating our findings, we suggest that in VSMCs and during vascular wound repair, $p21^{Cip1}$ is able to modulate vascular SDF-1 levels by inhibiting the binding of STAT3 to the SDF-1 promoter. Adding complexity, it has also recently been shown that $p21^{Cip1}$ is a direct STAT3 target, and furthermore, that STAT3 functions as a transcriptional repressor of p53, an important transcriptional activator of $p21^{Cip1}$ (65, 66). However, it is also known that STAT3 and HIF-1α form a complex that regulates VEGF transcription (52), thus the possibility exists that HIF-1α also participates in the regulation of SDF-1 via this higher order transcriptional complex. Therefore, considering all available data and reports, we consider the following possible in the context of vascular wound repair and remodeling: (a) A positive feedback loop for SDF-1 operates via JAK/STAT signaling in the early phase of this process. (b) A negative feedback loop controls STAT3 transcriptional activity through $p21^{Cip1}$, connecting the p53-mediated cellular stress response to the inflammatory response and restraining the latter in a $p21^{Cip1}$-dependent manner. (c) Medial VSMCs modulate the immune response to vascular injury by the synthesis and secretion of SDF-1.

Importantly, numerous aspects of this study are of clinical relevance. However, none is perhaps more obvious than the potential application of our findings to vascular stent technologies. Thus, we speculate that several of the important regulators of the vascular remodeling process that were identified in this study (or their inhibitors) may have potential clinical utility if appropriately loaded onto "drug-eluting" stents. Conceivably, this could be either as adjuncts to, or replacements for, either sirolimus or paxlitaxel, the agents commonly used for this purpose at the current time.

In conclusion, our findings indicate that $p21^{Cip1}$ plays an important role in the modulation of vascular remodeling after arterial injury. In local vascular cells, $p21^{Cip1}$ restrains proliferation and the inflammatory response during vascular wound repair. Under the influence of $p21^{Cip1}$, VSMC-derived SDF-1 plays a pivotal role in recruiting inflammatory cells to the injured area, and we propose that $p21^{Cip1}$ regulates SDF-1 via the JAK/STAT signaling pathway. Importantly, this provides a possible link between the p53/$p21^{Cip1}$-mediated cellular stress signaling program and the inflammatory response during vascular remodeling. Collectively, these findings suggest a central role for SDF-1 in vascular injury repair. We are cautiously optimistic that the targeted manipulation of key biologic regulators of the vascular repair process, in particular $p21^{Cip1}$ and the SDF-1/CXCR4 axis, may be useful clinical adjuncts in the treatment or primary prevention of atherosclerotic vascular disease.

## Methods

*Generation of homozygous mice.* Heterozygous 129/B6 *p21*$^{+/-}$ mice were obtained from Tyler Jacks (David H. Koch Institute for Integrative Cancer Research at MIT, Massachusetts Institute of Technology, Cambridge, Massachusetts, USA). All animal experiments were approved by the National Heart, Lung, and Blood Institute Animal Care and Use Committee. We back bred the mice for 12 generations against a C57BL/6 background and studied male and female mice at 10 weeks of age. *p21*$^{+/+}$ littermates were used as controls. Genotyping was performed by PCR amplification of mouse tail DNA using allele-specific probes. Each experimental group contained a minimum of 5 mice.

*Primary VSMCs, cell proliferation, and cellular stress response.* VSMCs were isolated by enzymatic and outgrowth methods (40), with careful attention given to the complete removal of the adventitial layer. Dissected pieces of aortic media were minced and incubated with collagenase (1 mg/ml) and elastase type III (0.125 mg/ml) in DMEM for 30 min. Tissues were plated with DMEM containing 10% FBS. Cell numbers were determined 24 to 96 hours later. Cellular stress was induced by incubating VSMCs with $H_2O_2$ at 375 μM and 750 μM for 1 hour. The apoptotic rate was determined 6 hours after incubation with $H_2O_2$. Apoptosis was induced with 10 and 50 ng/ml recombinant FasL (R&D Systems) for 12 hours in the presence of 10 μg/ml of a cross-linking antibody (mouse anti-6X histidine; R&D Systems). Annexin V staining was performed according to the manufacturer's protocol (BD Biosciences — Pharmingen). STAT3 activation and inhibition was performed in low-serum cultured (0.5% FBS) VSMCs. Cells were incubated with 40 ng/ml LIF (Sigma-Aldrich), and *SDF-1* mRNA expression was analyzed at the indicated time points. LIF-stimulated VSMCs were incubated with the STAT3 activation inhibitor PpYLKTK-mts (Calbiochem) at the indicated concentrations and *SDF-1* mRNA expression analyzed 4 hours later.

*Quantitative RT-PCR.* RNA was extracted from blood vessels using the Qiagen RNeasy kit. A total of 2 μg total RNA was annealed to 1 μg of random primers at 70°C, and first-strand cDNA synthesis was performed in a 25-μl reaction volume following the Promega protocol for M-MLV reverse transcriptase. $p21^{Cip1}$, p53, and SDF-1 expression levels were analyzed by real-time PCR using the DyNAmo HS SYBR Green qPCR kit (New England Biolabs Inc.), with 0.2 μl from each cDNA synthesis (or the equivalent cDNA from 15 ng of RNA) and a final primer concentration of 0.3 μM in each 20-μl PCR reaction. Real-time PCR was performed with an initial 10-min cycle at 95°C (denaturation), followed by 40 amplification cycles as follows: 10 s at 95°C (denaturation), 20 s at 60°C (annealing), and 30 s at 72°C (extension). Primer sequences are available in Supplemental Methods.

*Wire injury in mice.* *p21*$^{-/-}$ and *p21*$^{+/+}$ mice were investigated using an established model of femoral artery wire injury, which results in complete endothelial denudation (66). This procedure was performed by a surgeon who was blinded to the mouse genotype. BrdU (25 mg/kg) was injected at 24 hours and 1 hour prior to tissue harvest. The percent of BrdU-positive cells in the intima and intima/media area ratio were analyzed by computer-assisted morphometry ($n$ = 5 mice, 10 arteries/group). For each mouse, 4 sections were analyzed per artery.

*BM transplantation*. BM was obtained from 8- to 12-week-old $p21^{-/-}$ and $p21^{+/+}$ mice after euthanasia with $CO_2$. BM cell suspensions were flushed from femurs and tibias, filtered, and stored on ice until use. Recipient mice were lethally irradiated with 900 rads of whole-body irradiation and then received $5 \times 10^6$ unfractionated BM cells by intravenous tail vein injection. Successful engraftment was confirmed 12 weeks later by quantitative PCR for the presence or absence of $p21^{Cip1}$ or *Sry* to distinguish female and male BM cells ($n$ = 5 mice, 10 arteries/group).

*Immunohistochemistry, western-blot, and immunoprecipitation analysis and arterial cytokine concentrations*. Immunohistochemistry was performed on paraffin-embedded tissues using an ABC immunoperoxidase protocol including antigen retrieval. The following primary antibodies were used: anti–smooth muscle α-actin antibody (1:1000, 1A4; Roche), F4/80 antibody against macrophages (1:100, A3-1; Serotec), 7/4 antibody against neutrophils (1:10, 7/4; Cedarlane), CD3 antibody against T lymphocytes (1:100; DAKO Cytomation), and alkaline phosphatase-conjugated mouse monoclonal antibody against BrdU (1 U/ml; Roche). Immunofluorescence staining was performed on fresh frozen tissue sections without antigen retrieval. Methanol/acetone-fixed sections were stained with primary antibodies against SDF-1 (1:100; eBioscience), CD31 (1:100, MEC 13.3; BD Biosciences — Pharmingen), CD45 (1:50, 30-F11; eBioscience), F4/80 (1:100; Invitrogen), $p21^{Cip1}$ (1:50, ab2961; Abcam Inc.), p53 (1:50, sc-6243; Santa Cruz Biotechnology Inc.), and smooth muscle α-actin (FITC-conjugated) (1:100, 1A4; Sigma-Aldrich). Where appropriate, these were used in conjunction with Alexa Fluor 488– or Alexa Fluor 594–conjugated secondary antibodies (1:200 dilution; Invitrogen). Apoptotic vascular cells were identified by TUNEL assay. Images were acquired using either a Zeiss Axioskop plus light microscope with AxioVision V4.3 software or, for confocal microscopy, a Zeiss LSM 510 UV laser scanning confocal microscope system (Carl Zeiss GmbH). Cell counting (minimum 100 cells/section) was performed by a blinded member of our laboratory with extensive experience in both cell morphology and the techniques described above. Western blot analysis was performed on homogenized arterial and VSMC samples in RIPA lysis buffer using antibodies against mouse $p21^{Cip1}$ (sc397, 1:1000; Santa Cruz Biotechnology Inc.), STAT3 (1:1000; Cell Signaling Technology), and p-STAT3 (1:1000; Cell Signaling Technology). Each lane was loaded with 50 μg protein (Bradford assay). For immunoprecipitation, cells were lysed in NP-40 buffer (75 mM NaCl, 1.0% NP-40, 50 mM Tris, pH 8.0, and protease inhibitors). Cell lysate (200 μg) was incubated with the antibodies indicated in Figure 2A and Figure 8D and/or with isotype control IgG and analyzed by western blot. Arterial cytokine concentrations were measured using a mouse SearchLight Proteome Array (Pierce Biotechnology).

*CXCR4 in vivo inhibition*. Commencing 24 hours prior to vascular injury, a continuous 20-mg/ml dose of AMD3100 (Sigma-Aldrich) was administered to mice via osmotic minipump (Alzet) at a rate of 2 mg/wk for 2 weeks. CXCR4 blocking antibody (clone 2B11; BD Biosciences) was administered intravenously commencing 24 hours prior to vascular injury at 3-day intervals for 1 or 2 weeks at a dose of 20 μg. IgG2b rat isotype antibody was used as a control for this experiment (clone A95-1; BD Biosciences) (48).

*Immunophenotyping*. Peripheral blood was isolated from mice by cardiac puncture before and 7 days after injury. Complete blood cell counts were performed using a standard automated cell counting hematology analyzer (Cell-dyne 3500; Abbott). Automated image identification for cell counting was performed. Inflammatory cell phenotyping was performed using 200 μl of blood lysed with ACK buffer for 15 minutes, incubated with Fc Block (BD Biosciences — Pharmingen), and then stained with fluorochrome-conjugated antibodies against CD11b (M1/70), CD62L (2.4G2), and Ly-6C/G (RB6-8C5) (all BD Biosciences — Pharmingen) for 30 minutes. We gated monocytes as $CD11b^+$ and side-scatter low and determined the percentage of Ly-$6C/G^+/CD62L^+$ and Ly-$6C/G^-/CD62L^-$ monocytes. Automatic compensation was performed based on single-stained samples for the respective antibodies. The stained cells were analyzed on a BD FACSCanto using Diva Software.

*Quantitative chromatin immunoprecipitation*. Formalin-crosslinked protein-DNA complexes in cell and tissue lysates were sonicated to an average size of ~500 bp. Complexes were pre-cleared and immunoprecipitated using protein A/G agarose beads (Zymed Laboratories) and a STAT3 antibody (Santa Cruz Biotechnology Inc.) or isotype controls. Subsequently, cross-linking was reversed by overnight incubation at 65°C and proteinase K treatment. The enriched specific promoter fragments were measured by quantitative PCR. SDF-1 primer sequences are available in Supplemental Methods. The relative SDF-1 promoter occupancy was adjusted to the background content of the unrelated β-actin promoter sequence, isotype IgG controls, and the initial sonicated chromatin input.

*Luciferase assays*. The potential STAT consensus sequence (TTCCCGGGAA) within the SDF-1 promoter was mutated to AGCCCGGGCT (SDF-mut) using the Quickchange mutagenesis II kit (Stratagene). Murine $p21^{-/-}$ and $p21^{+/+}$ VSMCs were transfected with 2 μg of the indicated plasmids (pGL3 backbone) and a control pRL-SV40 plasmid using the Amaxa Nucleofactor Kit (Amaxa) according to the manufacturer's instructions. Luciferase activity was quantified 24 hours after transfection using the dual luciferase assay system (Promega) and was normalized to the expression of *Renilla* luciferase.

*Statistics*. Numbers of mice used for each experiment are provided in the figure legends. For cell culture and immunohistochemistry, each individual experiment was repeated 3 times. Experimental data were analyzed by ANOVA followed by Dunn correction or unpaired 2-tailed $t$ test. Results are expressed as mean ± SEM.

## Acknowledgments

We thank Tyler Jacks for kindly providing the $p21^{Cip1}$ knockout mice and Giovanna Tosato for sharing reagents. We thank the staff of the Laboratory of Animal Medicine and Surgery and Robin Schwartzbeck for their assistance with the transgenic mice. We also acknowledge the professional skills and advice of Christian A. Combs and Daniela Malide (Light Microscopy Core Facility, National Heart, Lung and Blood Institute) and J. Philip McCoy (Flow Cytometry Core Facility, National Heart, Lung and Blood Institute). This project was funded by the intramural research program of the National Heart, Lung, and Blood Institute.

Received for publication December 15, 2006, and accepted in revised form March 17, 2008.

Address correspondence to: Manfred Boehm, Building 10-CRC, Room 5-3132, Cardiovascular Branch, National Heart, Lung, and Blood Institute, NIH, Bethesda, Maryland 20817, USA. Phone: (301) 435-7211; Fax: (301) 451-7090; E-mail: boehmm@nhlbi.nih.gov.

1. Libby, P. 2002. Inflammation in atherosclerosis. *Nature*. **420**:868–874.
2. Binder, C.J., et al. 2002. Innate and acquired immunity in atherogenesis. *Nat. Med.* **8**:1218–1226.
3. Sata, M., et al. 2002. Hematopoietic stem cells differentiate into vascular cells that participate in the pathogenesis of atherosclerosis. *Nat. Med.* **8**:403–409.
4. Boehm, M., et al. 2004. Bone marrow-derived immune cells regulate vascular disease through a p27(Kip1)-dependent mechanism. *J. Clin. Invest.* **114**:419–426.
5. Grunewald, M., et al. 2006. VEGF-induced adult neovascularization: recruitment, retention, and role of accessory cells. *Cell.* **124**:175–189.
6. Chen, S., et al. 2005. Transforming growth factor-beta1 increases CXCR4 expression, stromal-derived factor-1alpha-stimulated signalling and human immunodeficiency virus-1 entry in human monocyte-

derived macrophages. *Immunology.* **114**:565–574.
7. Busillo, J.M., and Benovic, J.L. 2007. Regulation of CXCR4 signaling. *Biochim. Biophys. Acta.* **1768**:952–963.
8. Schecter, A.D., Berman, A.B., and Taubman, M.B. 2003. Chemokine receptors in vascular smooth muscle. *Microcirculation.* **10**:265–272.
9. Vila-Coro, A.J., et al. 1999. The chemokine SDF-1alpha triggers CXCR4 receptor dimerization and activates the JAK/STAT pathway. *FASEB J.* **13**:1699–1710.
10. Moepps, B., et al. 1997. Two murine homologues of the human chemokine receptor CXCR4 mediating stromal cell-derived factor 1alpha activation of Gi2 are differentially expressed in vivo. *Eur. J. Immunol.* **27**:2102–2112.
11. Sherr, C.J., and Roberts, J.M. 1999. CDK inhibitors: positive and negative regulators of G1-phase progression. *Genes Dev.* **13**:1501–1512.
12. Sherr, C.J., and Roberts, J.M. 2004. Living with or without cyclins and cyclin-dependent kinases. *Genes Dev.* **18**:2699–2711.
13. el-Deiry, W.S., et al. 1993. WAF1, a potential mediator of p53 tumor suppression. *Cell.* **75**:817–825.
14. Gu, Y., Turck, C.W., and Morgan, D.O. 1993. Inhibition of CDK2 activity in vivo by an associated 20K regulatory subunit. *Nature.* **366**:707–710.
15. Harper, J.W., Adami, G.R., Wei, N., Keyomarsi, K., and Elledge, S.J. 1993. The p21 Cdk-interacting protein Cip1 is a potent inhibitor of G1 cyclin-dependent kinases. *Cell.* **75**:805–816.
16. Xiong, Y., et al. 1993. p21 is a universal inhibitor of cyclin kinases. *Nature.* **366**:701–704.
17. Suzuki, A., Tsutomi, Y., Akahane, K., Araki, T., and Miura, M. 1998. Resistance to Fas-mediated apoptosis: activation of caspase 3 is regulated by cell cycle regulator p21WAF1 and IAP gene family ILP. *Oncogene.* **17**:931–939.
18. Cheng, M., et al. 1999. The p21(Cip1) and p27(Kip1) CDK 'inhibitors' are essential activators of cyclin D-dependent kinases in murine fibroblasts. *EMBO J.* **18**:1571–1583.
19. LaBaer, J., et al. 1997. New functional activities for the p21 family of CDK inhibitors. *Genes Dev.* **11**:847–862.
20. Seoane, J., Le, H.V., and Massague, J. 2002. Myc suppression of the p21(Cip1) Cdk inhibitor influences the outcome of the p53 response to DNA damage. *Nature.* **419**:729–734.
21. Merched, A.J., and Chan, L. 2004. Absence of p21Waf1/Cip1/Sdi1 modulates macrophage differentiation and inflammatory response and protects against atherosclerosis. *Circulation.* **110**:3830–3841.
22. Scatizzi, J.C., et al. 2006. p21Cip1 is required for the development of monocytes and their response to serum transfer-induced arthritis. *Am. J. Pathol.* **168**:1531–1541.
23. Chang, M.W., Barr, E., Lu, M.M., Barton, K., and Leiden, J.M. 1995. Adenovirus-mediated overexpression of the cyclin/cyclin-dependent kinase inhibitor, p21 inhibits vascular smooth muscle cell proliferation and neointima formation in the rat carotid artery model of balloon angioplasty. *J. Clin. Invest.* **96**:2260–2268.
24. Condorelli, G., Aycock, J.K., Frati, G., and Napoli, C. 2001. Mutated p21/WAF/CIP transgene overexpression reduces smooth muscle cell proliferation, macrophage deposition, oxidation-sensitive mechanisms, and restenosis in hypercholesterolemic apolipoprotein E knockout mice. *FASEB J.* **15**:2162–2170.
25. Sata, M., et al. 2002. Mouse genetic evidence that tranilast reduces smooth muscle cell hyperplasia via a p21(WAF1)-dependent pathway. *Arterioscler. Thromb. Vasc. Biol.* **22**:1305–1309.
26. Yang, Z.Y., et al. 1996. Role of the p21 cyclin-dependent kinase inhibitor in limiting intimal cell proliferation in response to arterial injury. *Proc. Natl. Acad. Sci. U. S. A.* **93**:7905–7910.
27. Tanner, F.C., et al. 2000. Differential effects of the cyclin-dependent kinase inhibitors p27(Kip1), p21(Cip1), and p16(Ink4) on vascular smooth muscle cell proliferation. *Circulation.* **101**:2022–2025.
28. Otterbein, L.E., et al. 2003. Carbon monoxide suppresses arteriosclerotic lesions associated with chronic graft rejection and with balloon injury. *Nat. Med.* **9**:183–190.
29. Diez-Juan, A., et al. 2004. Selective inactivation of p27(Kip1) in hematopoietic progenitor cells increases neointimal macrophage proliferation and accelerates atherosclerosis. *Blood.* **103**:158–161.
30. Moses, J.W., et al. 2003. Sirolimus-eluting stents versus standard stents in patients with stenosis in a native coronary artery. *N. Engl. J. Med.* **349**:1315–1323.
31. Suzuki, T., et al. 2001. Stent-based delivery of sirolimus reduces neointimal formation in a porcine coronary model. *Circulation.* **104**:1188–1193.
32. Mancini, D., et al. 2003. Use of rapamycin slows progression of cardiac transplantation vasculopathy. *Circulation.* **108**:48–53.
33. Carter, A.J., et al. 2004. Long-term effects of polymer-based, slow-release, sirolimus-eluting stents in a porcine coronary model. *Cardiovasc. Res.* **63**:617–624.
34. Perkins, N.D. 2002. Not just a CDK inhibitor: regulation of transcription by p21(WAF1/CIP1/SDI1). *Cell Cycle.* **1**:39–41.
35. Coqueret, O. 2003. New roles for p21 and p27 cell-cycle inhibitors: a function for each cell compartment? *Trends Cell Biol.* **13**:65–70.
36. Kitaura, H., et al. 2000. Reciprocal regulation via protein-protein interaction between c-Myc and p21(cip1/waf1/sdi1) in DNA replication and transcription. *J. Biol. Chem.* **275**:10477–10483.
37. Coqueret, O., and Gascan, H. 2000. Functional interaction of STAT3 transcription factor with the cell cycle inhibitor p21WAF1/CIP1/SDI1. *J. Biol. Chem.* **275**:18794–18800.
38. Delavaine, L., and La Thangue, N.B. 1999. Control of E2F activity by p21Waf1/Cip1. *Oncogene.* **18**:5381–5392.
39. Harris, T.E., Albrecht, J.H., Nakanishi, M., and Darlington, G.J. 2001. CCAAT/enhancer-binding protein-alpha cooperates with p21 to inhibit cyclin-dependent kinase-2 activity and induces growth arrest independent of DNA binding. *J. Biol. Chem.* **276**:29200–29209.
40. Tanner, F.C., et al. 1998. Expression of cyclin-dependent kinase inhibitors in vascular disease. *Circ. Res.* **82**:396–403.
41. Bruhl, T., et al. 2004. p21Cip1 levels differentially regulate turnover of mature endothelial cells, endothelial progenitor cells, and in vivo neovascularization. *Circ. Res.* **94**:686–692.
42. Maejima, Y., et al. 2003. Nitric oxide inhibits ischemia/reperfusion-induced myocardial apoptosis by modulating cyclin A-associated kinase activity. *Cardiovasc. Res.* **59**:308–320.
43. Zhang, C., Kavurma, M.M., Lai, A., and Khachigian, L.M. 2003. Ets-1 protects vascular smooth muscle cells from undergoing apoptosis by activating p21WAF1/Cip1: ETS-1 regulates basal and and inducible p21WAF1/Cip: ETS-1 regulates basal and inducible p21WAF1/Cip1 transcription via distinct cis-acting elements in the p21WAF/Cip1 promoter. *J. Biol. Chem.* **278**:27903–27909.
44. Beuvink, I., et al. 2005. The mTOR inhibitor RAD001 sensitizes tumor cells to DNA-damaged induced apoptosis through inhibition of p21 translation. *Cell.* **120**:747–759.
45. Duckers, H.J., et al. 2001. Heme oxygenase-1 protects against vascular constriction and proliferation. *Nat. Med.* **7**:693–698.
46. Aiuti, A., Webb, I.J., Bleul, C., Springer, T., and Gutierrez-Ramos, J.C. 1997. The chemokine SDF-1 is a chemoattractant for human CD34+ hematopoietic progenitor cells and provides a new mechanism to explain the mobilization of CD34+ progenitors to peripheral blood. *J. Exp. Med.* **185**:111–120.
47. Kovacic, J.C., Muller, D.W., and Graham, R.M. 2007. Actions and therapeutic potential of G-CSF and GM-CSF in cardiovascular disease. *J. Mol. Cell. Cardiol.* **42**:19–33.
48. Jin, D.K., et al. 2006. Cytokine-mediated deployment of SDF-1 induces revascularization through recruitment of CXCR4+ hemangiocytes. *Nat. Med.* **12**:557–567.
49. Shiba, Y., et al. 2007. M-CSF accelerates neointimal formation in the early phase after vascular injury in mice: the critical role of the SDF-1-CXCR4 system. *Arterioscler. Thromb. Vasc. Biol.* **27**:283–289.
50. Moskovits, N., Kalinkovich, A., Bar, J., Lapidot, T., and Oren, M. 2006. p53 Attenuates cancer cell migration and invasion through repression of SDF-1/CXCL12 expression in stromal fibroblasts. *Cancer Res.* **66**:10671–10676.
51. Mehta, S.A., et al. 2007. Negative regulation of chemokine receptor CXCR4 by tumor suppressor p53 in breast cancer cells: implications of p53 mutation or isoform expression on breast cancer cell invasion. *Oncogene.* **26**:3329–3337.
52. Jung, J.E., et al. 2005. STAT3 is a potential modulator of HIF-1-mediated VEGF expression in human renal carcinoma cells. *FASEB J.* **19**:1296–1298.
53. Funamoto, M., et al. 2000. Signal transducer and activator of transcription 3 is required for glycoprotein 130-mediated induction of vascular endothelial growth factor in cardiac myocytes. *J. Biol. Chem.* **275**:10561–10566.
54. Davis, C., Fischer, J., Ley, K., and Sarembock, I.J. 2003. The role of inflammation in vascular injury and repair. *J. Thromb. Haemost.* **1**:1699–1709.
55. Walsh, K., Smith, R.C., and Kim, H.S. 2000. Vascular cell apoptosis in remodeling, restenosis, and plaque rupture. *Circ. Res.* **87**:184–188.
56. Granada, J.F., et al. 2005. Single perivascular delivery of mitomycin C stimulates p21 expression and inhibits neointima formation in rat arteries. *Arterioscler. Thromb. Vasc. Biol.* **25**:2343–2348.
57. Smith, R.C., et al. 1997. p21CIP1-mediated inhibition of cell proliferation by overexpression of the gax homeodomain gene. *Genes Dev.* **11**:1674–1689.
58. De Clercq, E. 2003. The bicyclam AMD3100 story. *Nat. Rev. Drug Discov.* **2**:581–587.
59. Nuhrenberg, T.G., et al. 2005. Rapamycin attenuates vascular wall inflammation and progenitor cell promoters after angioplasty. *FASEB J.* **19**:246–248.
60. Togel, F., Isaac, J., Hu, Z., Weiss, K., and Westenfelder, C. 2005. Renal SDF-1 signals mobilization and homing of CXCR4-positive cells to the kidney after ischemic injury. *Kidney Int.* **67**:1772–1784.
61. Butler, J.M., et al. 2005. SDF-1 is both necessary and sufficient to promote proliferative retinopathy. *J. Clin. Invest.* **115**:86–93.
62. Abbott, J.D., et al. 2004. Stromal cell-derived factor-1alpha plays a critical role in stem cell recruitment to the heart after myocardial infarction but is not sufficient to induce homing in the absence of injury. *Circulation* **110**:3300–3305.
63. Zernecke, A., et al. 2005. SDF-1alpha/CXCR4 axis is instrumental in neointimal hyperplasia and recruitment of smooth muscle progenitor cells. *Circ. Res.* **96**:784–791.
64. Karshovska, E., et al. 2007. Expression of HIF-1alpha in injured arteries controls SDF-1alpha mediated neointima formation in apolipoprotein E deficient mice. *Arterioscler. Thromb. Vasc. Biol.* **27**:2540–2547.
65. Giraud, S., Hurlstone, A., Avril, S., and Coqueret, O. 2004. Implication of BRG1 and cdk9 in the STAT3-mediated activation of the p21waf1 gene. *Oncogene.* **23**:7391–7398.
66. Niu, G., et al. 2005. Role of Stat3 in regulating p53 expression and function. *Mol. Cell. Biol.* **25**:7432–7440.